YMTHE, Volume *29*

Supplemental Information

Restoring neuronal chloride homeostasis with anti-NKCC1 gene therapy rescues cognitive deficits in a mouse model of Down syndrome

Martina Parrini, Shovan Naskar, Micol Alberti, Ilaria Colombi, Giovanni Morelli, Anna Rocchi, Marina Nanni, Federica Piccardi, Severine Charles, Giuseppe Ronzitti, Federico Mingozzi, Andrea Contestabile, and Laura Cancedda

A

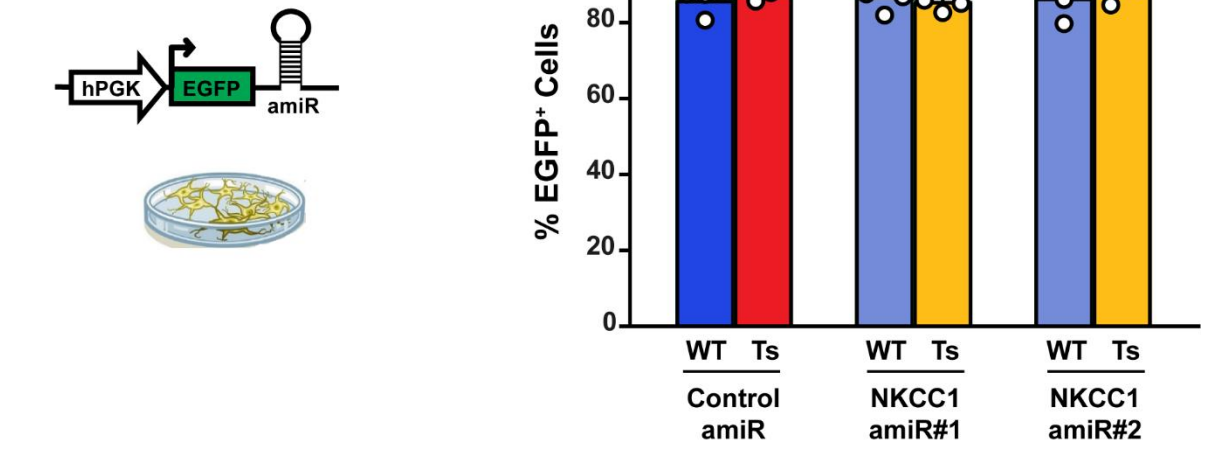
hPGK-EGFP-amiR LV Vector
hPGK
EGFP
amiR
% EGFP+ Cells
100
80
60
40
20
0
WT Ts
Control amiR
WT Ts
NKCC1 amiR#1
WT Ts
NKCC1 amiR#2

B

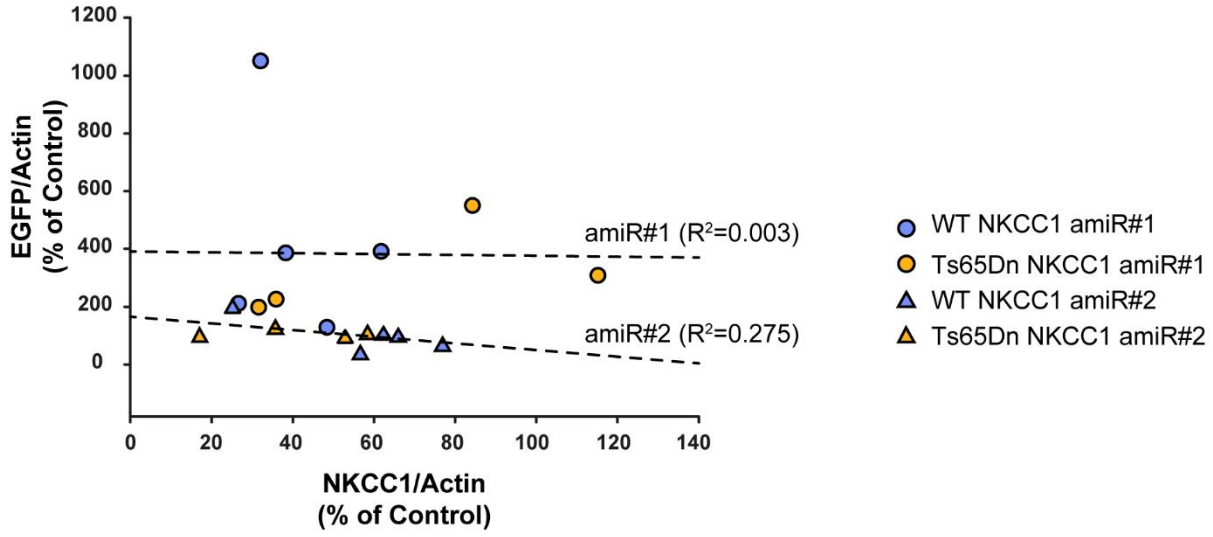
EGFP/Actin (% of Control)
1200
1000
800
600
400
200
0
amiR#1 (R²=0.003)
amiR#2 (R²=0.275)
0
20
40
60
80
100
120
140
NKCC1/Actin (% of Control)
WT NKCC1 amiR#1
Ts65Dn NKCC1 amiR#1
WT NKCC1 amiR#2
Ts65Dn NKCC1 amiR#2

Supplementary Figure 1. Infection efficiency and GFP expression in LV-transduced neurons in culture **(A)** *Left:* Schematic representation of the LV vector used for transducing neuronal cultures. *Right:* Quantification of the percentage of EGFP-positive ($EGFP^+$) cells in 15DIV infected neuronal cultures. **(B)** Scatterplot representation of NKCC1 and EGFP protein expression for each individual cell culture sample upon NKCC1 knockdown (amiR#1 and amiR#2). Correlation between EGFP expression and NKCC1 knockdown efficiency was lower for amiR#1 compared to amiR#2 as shown by the R^2 estimation of goodness-of-fit of the linear regression (dotted lines). Similarly, statistical relationship between EGFP and NKCC1 expression was actually lower for amiR#1 (Pearson correlation coefficient -0.016) compared to amiR#2 (Pearson correlation coefficient -0.524). However, no significantly correlation between EGFP expression and NKCC1 knockdown efficiency was found for either amiR#1 (P = 0.968) or amiR#2 (P = 0.147). Data in A are means (± SEM), dots indicate values of individual cell culture samples, obtained from 2 independent neuronal cultures. In B, dots and triangles indicate individual cell culture sample obtained from 5 independent neuronal cultures (same samples shown in Fig. 1B).

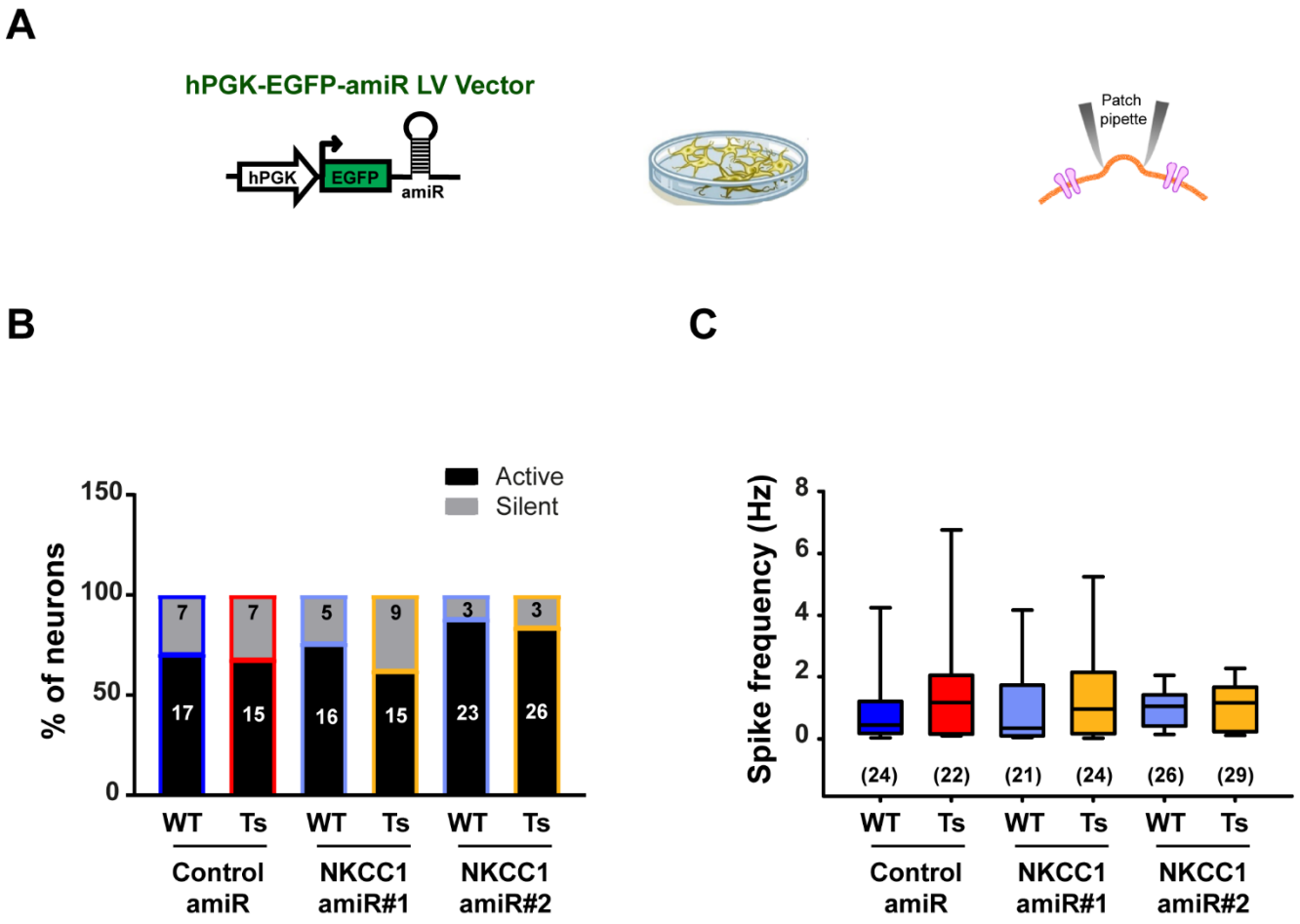

Supplementary Figure 2. Similar spontaneous spiking activity in LV-transduced WT and Ts65Dn hippocampal neurons in cultures recorded by patch-clamp. (A) *Left:* Schematic representation of the lentiviral vector (LV) expressing either control or NKCC1 amiRs. *Right:* LV-transduced hippocampal neurons in culture from WT and Ts65Dn mice (16-20 DIV) were recorded in cell-attached, patch-clamp configuration. **(B)** Percentage of spontaneously active hippocampal neurons in culture during baseline recordings for the diverse experimental groups. Numbers inside the bars indicate the number of recorded cells that were either active or silent during baseline recordings. No significant difference was found between groups by Fisher's exact test. **(C)** Quantification of the spontaneous spiking frequency recorded during baseline assessment of all recorded LV-transduced hippocampal neurons in culture. No significant difference was found between groups by two-way ANOVA followed by Tukey *post hoc* test. Data are means (± SEM), Box plots indicate median and 25^{th}-75^{th} percentiles and whiskers represent the 5^{th}-95^{th} percentiles. Number in parenthesis indicate number of recorded cells for each experimental group. Results shown in this figure represent the pooled data obtained from baseline recordings of cells shown in Fig. 2B and 2D.

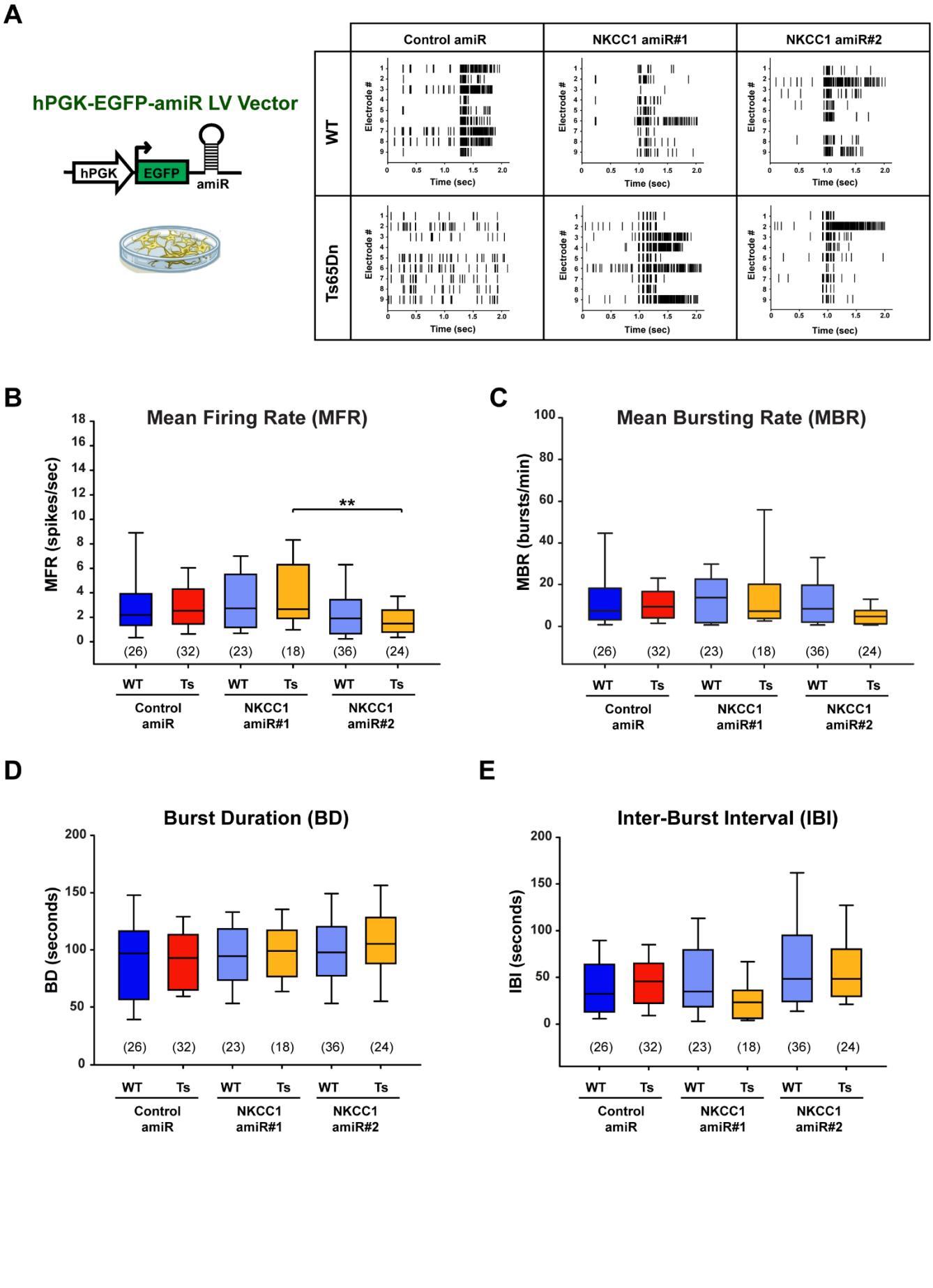
A
hPGK-EGFP-amiR LV Vector
hPGK
EGFP
amiR
Control amiR
NKCC1 amiR#1
NKCC1 amiR#2
WT
Ts65Dn
Electrode #
Time (sec)
B
Mean Firing Rate (MFR)
MFR (spikes/sec)
**
C
Mean Bursting Rate (MBR)
MBR (bursts/min)
D
Burst Duration (BD)
BD (seconds)
E
Inter-Burst Interval (IBI)
IBI (seconds)
(26) (32) (23) (18) (36) (24)
WT Ts WT Ts WT Ts
Control amiR
NKCC1 amiR#1
NKCC1 amiR#2

Supplementary Figure 3. Similar firing and bursting activity in LV-transduced WT and Ts65Dn neurons in cultures recorded on MEAs. (A) Representative raster-plots showing spontaneous activity of LV-transduced WT and Ts65Dn hippocampal cultures at 21 DIV recorded by MEAs. Note reduced correlated activity across electrodes in Ts65Dn neurons transduced with control amiR. **(B)** Quantification of the spontaneous mean firing rate (MFR) of LV-transduced WT and Ts65Dn neurons recorded by MEAs. **(C)** Quantification of the spontaneous mean bursting rate (MBR) of LV-transduced WT and Ts65Dn neurons recorded by MEAs. **(D)** Mean burst duration of individual MEAs seeded with LV-transduced WT and Ts65Dn neurons. **(E)** Mean inter-burst duration of individual MEAs seeded with LV-transduced WT and Ts65Dn neurons. Box plots indicate median and 25^{th}-75^{th} percentiles, whiskers represent the 5^{th}-95^{th} percentiles. Number in parenthesis indicates the number of MEA analyzed (obtained from 9 independent neuronal cultures). $^{**}P<0.01$, Tukey *post hoc* test following two-way ANOVA.

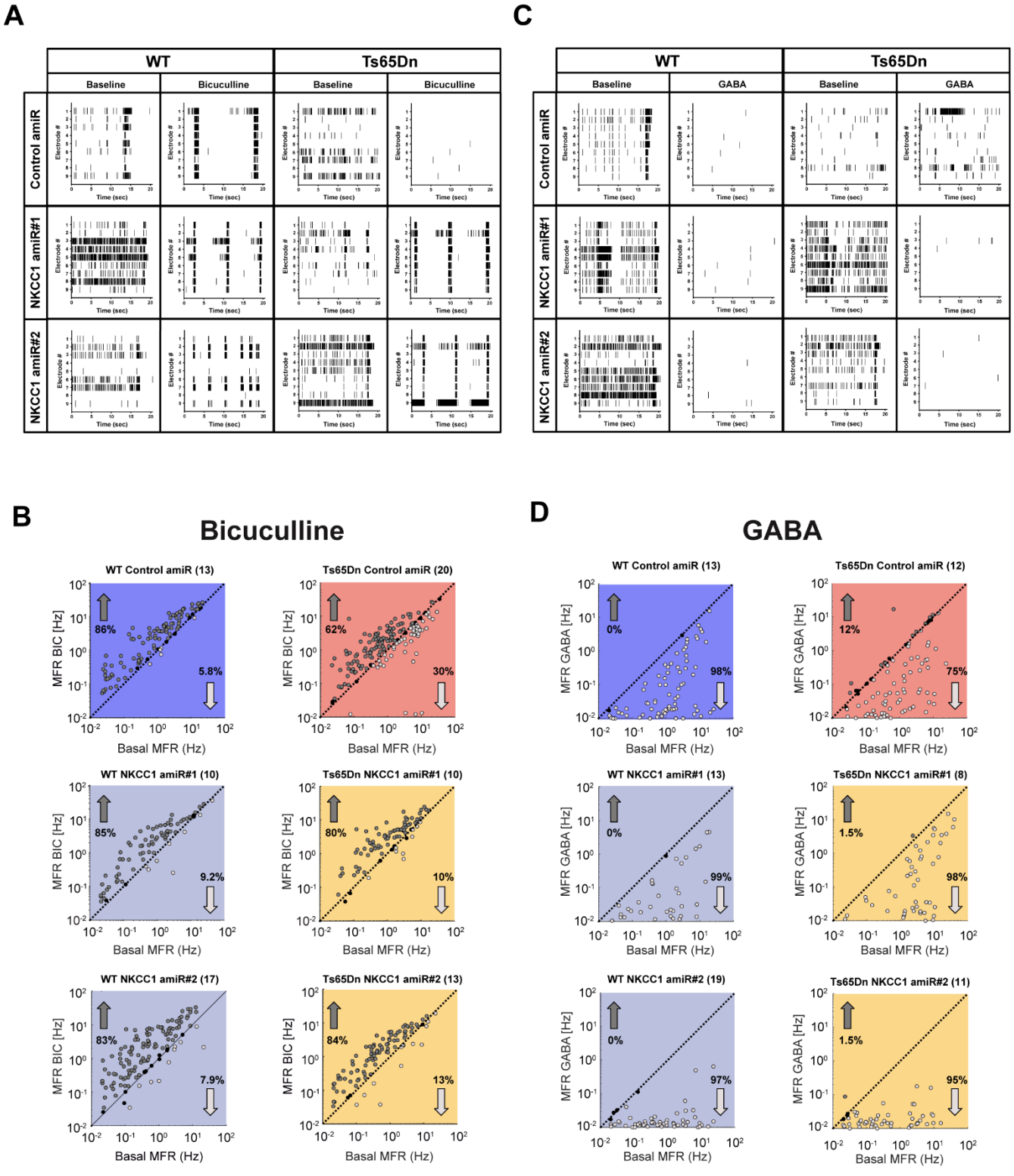
A
WT
Ts65Dn
Baseline
Bicuculline
Control amiR
NKCC1 amiR#1
NKCC1 amiR#2
Electrode #
Time (sec)
C
WT
Ts65Dn
Baseline
GABA
Control amiR
NKCC1 amiR#1
NKCC1 amiR#2
Electrode #
Time (sec)
B
Bicuculline
WT Control amiR (13)
86%
5.8%
Ts65Dn Control amiR (20)
62%
30%
WT NKCC1 amiR#1 (10)
85%
9.2%
Ts65Dn NKCC1 amiR#1 (10)
80%
10%
WT NKCC1 amiR#2 (17)
83%
7.9%
Ts65Dn NKCC1 amiR#2 (13)
84%
13%
MFR BIC [Hz]
Basal MFR (Hz)
D
GABA
WT Control amiR (13)
0%
98%
Ts65Dn Control amiR (12)
12%
75%
WT NKCC1 amiR#1 (13)
0%
99%
Ts65Dn NKCC1 amiR#1 (8)
1.5%
98%
WT NKCC1 amiR#2 (19)
0%
97%
Ts65Dn NKCC1 amiR#2 (11)
1.5%
95%
MFR GABA [Hz]
Basal MFR (Hz)

Supplementary Figure 4. Anti NKCC1 amiR treatment rescues neuronal-network inhibitory GABAergic signaling in Ts65Dn cultures. (A) Representative raster-plots showing firing activity of LV-transduced WT and Ts65Dn hippocampal cultures at 21 DIV recorded with MEAs before and after bath application of the $GABA_AR$ antagonist bicuculline (20 μM). For Ts65Dn neurons transduced with control amiR, example MEA recording shows decreased firing after bicuculline treatment. Increase in firing following bicuculline application was restored in Ts65Dn neurons by NKCC1 knockdown. **(B)** Scatter plots showing MFR for each active electrode (plotted as a dot) from all recorded MEAs seeded with WT and Ts65Dn neurons before (*x*-axis) and after (*y*-axis) bath application of bicuculline (the same data are presented as average in Main Figure 3E). Significant changes in MFR for each electrode upon bicuculline application was evaluated by bootstrap analysis. Dark-grey dots indicate electrodes showing a significant increase in MFR. Light-grey dots indicate electrodes showing a significant decrease in the MFR. Black dots indicate electrodes showing no significant changes in MFR. **(C)** Representative raster-plots showing firing activity of LV-transduced WT and Ts65Dn hippocampal cultures at 21 DIV recorded with MEAs before and after bath application of GABA (20 μM). WT neurons showed a sharp decrease in firing in all tested conditions. For Ts65Dn neurons transduced with control amiR, example MEA recording shows increased firing upon GABA treatment. GABA-mediated inhibition was restored in Ts65Dn neurons upon NKCC1 knockdown. **(D)** Scatter plots showing MFR for each active electrode (plotted as a dot) from all recorded MEAs seeded with WT and Ts65Dn neurons before (*x*-axis) and after (*y*-axis) bath application of GABA (the same data are presented as average in Main Figure 3G). Significant changes in MFR for each electrode upon GABA application was evaluated by bootstrap analysis. Dark-grey dots indicate electrodes showing a significant increase in MFR. Light-grey dots indicate electrodes showing a significant decrease in the MFR. Black dots indicate electrodes showing no significant changes in MFR. In B and D, numbers in parenthesis indicate the number of analyzed MEA (obtained from 9 independent neuronal cultures), whereas arrows and numbers in the boxes indicate the percentage of electrodes showing a significant increase (↑) or decrease (↓) in MFR by bootstrap analysis.

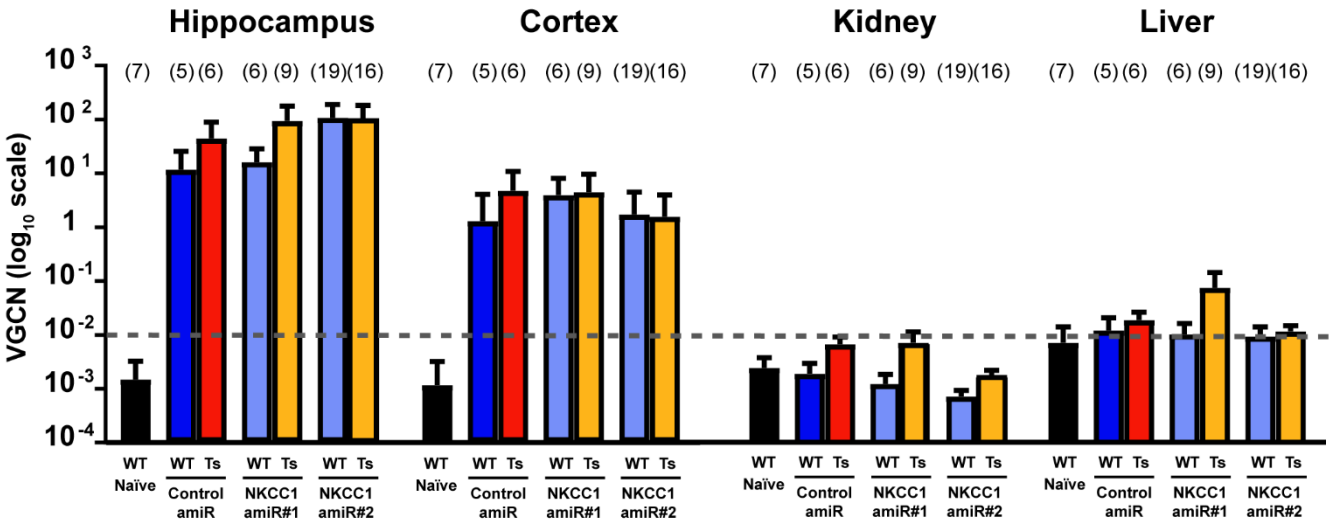

Supplementary Figure 5. AAV_9 bio-distribution analysis in brain and peripheral organs. Bio-distribution analysis of viral vector genome copy number (VGCN; copies/cell) by real-time quantitative PCR (qPCR) in brains of WT and Ts65Dn mice 6 weeks post-injection showed higher VGCN in the hippocampus compared to cortex (logarithmic scale). VGCN from hippocampus and cortex of WT non-injected (naïve) mice were below detection limit of the assay (0.01 copies/cell; dotted line). Similarly, VGCN were undetectable in kidney while traces only were found in the liver of AVV_9-injected WT and Ts65Dn mice. Numbers in parenthesis indicate the number of sample analyzed for each experimental group.

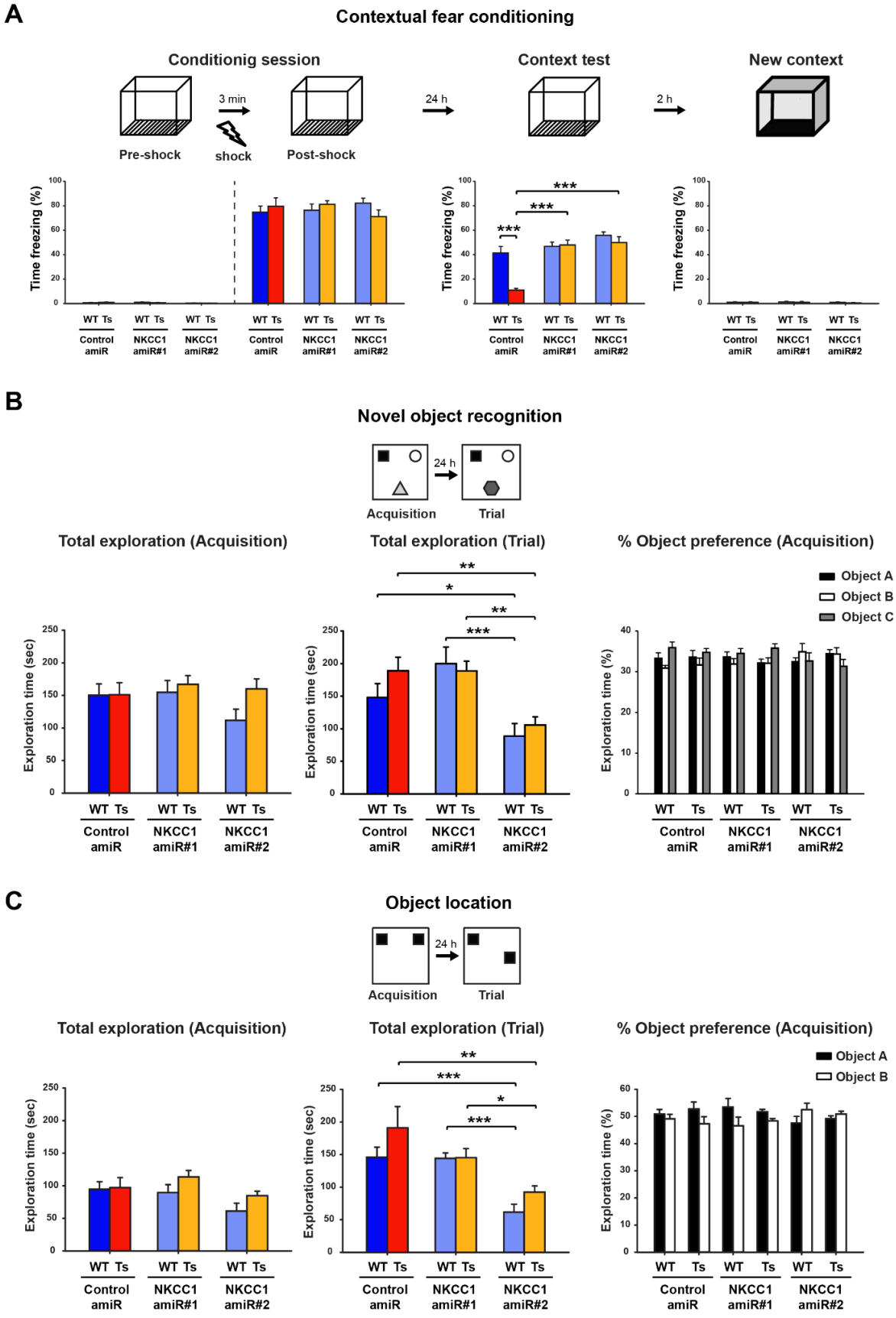
A
Contextual fear conditioning
Conditionig session
Context test
New context
3 min
24 h
2 h
Pre-shock
shock
Post-shock
Time freezing (%)
WT Ts
Control amiR
NKCC1 amiR#1
NKCC1 amiR#2
***
B
Novel object recognition
24 h
Acquisition
Trial
Total exploration (Acquisition)
Total exploration (Trial)
% Object preference (Acquisition)
Exploration time (sec)
Exploration time (%)
**
*
***
Object A
Object B
Object C
C
Object location
24 h
Acquisition
Trial
Total exploration (Acquisition)
Total exploration (Trial)
% Object preference (Acquisition)
Exploration time (sec)
Exploration time (%)
**
***
*
***
Object A
Object B

Supplementary Figure 6. Effect of AAV_9 delivery of control and NKCC1 amiRs on behavioral tasks at 6 weeks post injection. (A) *Left:* in the CFC test, brain AAV_9 delivery had no effect on the freezing time before (left) or immediately after (right) the electric foot shock during the conditioning session in both WT and Ts65Dn mice. *Center*: quantification of the freezing response in AAV_9-injected WT and Ts65Dn mice when re-exposed to the conditioning context (same data showed in Fig 4C). *Right:* both WT and Ts65Dn mice showed negligible freezing response when exposed to a new context. Control amiR: WT, *n* = 10; Ts65Dn, *n* = 10. NKCC1 amiR#1: WT, *n* = 10; Ts65Dn, *n* = 10. NKCC1 amiR#2: WT, *n* = 9; Ts65Dn, *n* = 9. **(B)** *Left*: in the NOR test the total exploration time during the acquisition phases was not significantly different across genotype and treatment. *Center*: the total exploration time during the trial phase was slightly decreased in both WT and Ts65Dn mice injected with AAV_9 expressing amiR#2, however no significant difference was observed in Ts65Dn mice compared to WT. *Right*: the percentage of time spent exploring the three objects during the acquisition phase of the NOR test was not statistically different across the experimental groups. Control amiR: WT, *n* = 9; Ts65Dn, *n* = 10. NKCC1 amiR#1: WT, *n* = 11; Ts65Dn, *n* = 10. NKCC1 amiR#2: WT, *n* = 11; Ts65Dn, *n* = 10. **(C)** *Left*: in the OL test the total exploration time during the acquisition phase was not significantly different across genotype and treatment. *Center*: the total exploration time during the trial phase was slightly decreased in both WT and Ts65Dn mice injected with AAV_9 expressing amiR#2, however no significant difference was observed in Ts65Dn mice compared to WT. *Right*: the percentage of time spent exploring the two objects during the acquisition phase of the OL test was not statistically different across the experimental groups. Control amiR: WT, *n* = 7; Ts65Dn, *n* = 10. NKCC1 amiR#1: WT, *n* = 7; Ts65Dn, *n* = 10. NKCC1 amiR#2: WT, *n* = 11; Ts65Dn, *n* = 9. For all panels: **P*<0.05, ***P*<0.01, ****P*<0.001, Tukey *post hoc* test following two-way ANOVA.

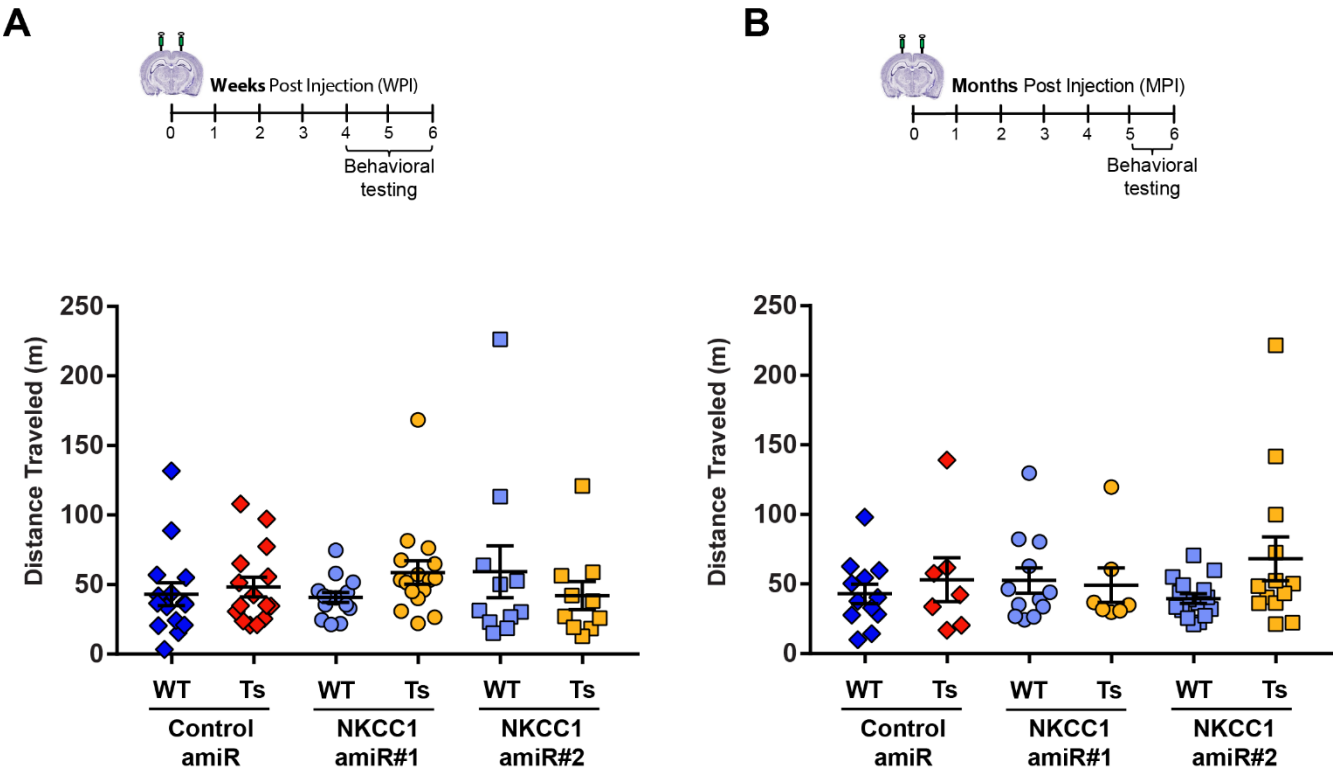

Supplementary Figure 7. Brain AAV$_9$ delivery of control and NKCC1 amiRs had no effect on mice motor activity. (A) *Top:* Schematic representation of the experimental timeline: 2-3 month-old WT and Ts65Dn mice were stereotaxically injected in the hippocampal CA1 region with AAV$_9$ vectors expressing EGFP and control or NKCC1 amiRs and analyzed 4-6 weeks later. *Bottom*: Motor activity was evaluated by measuring the distance traveled by mice in the empty arena. Distance traveled was not significantly different across genotypes and treatments. Control amiR: WT, *n* = 15; Ts65Dn, *n* = 15. NKCC1 amiR#1: WT, *n* = 15; Ts65Dn, *n* = 16. NKCC1 amiR#2: WT, *n* = 10; Ts65Dn, *n* = 11. **(B)** *Top:* Schematic representation of the experimental timeline: 2-3 month-old WT and Ts65Dn mice were stereotaxically injected in the hippocampal CA1 region with AAV$_9$ vectors expressing EGFP and control or NKCC1 amiRs and analyzed 5-6 months later. *Bottom*: Distance traveled was not significantly different across genotypes and treatments. Control amiR: WT, *n* = 12; Ts65Dn, *n* = 7. NKCC1 amiR#1: WT, *n* = 12; Ts65Dn, *n* = 7. NKCC1 amiR#2: WT, *n* = 16; Ts65Dn, *n* = 13. Symbols indicate values from single animals; lines report group averages (± SEM).

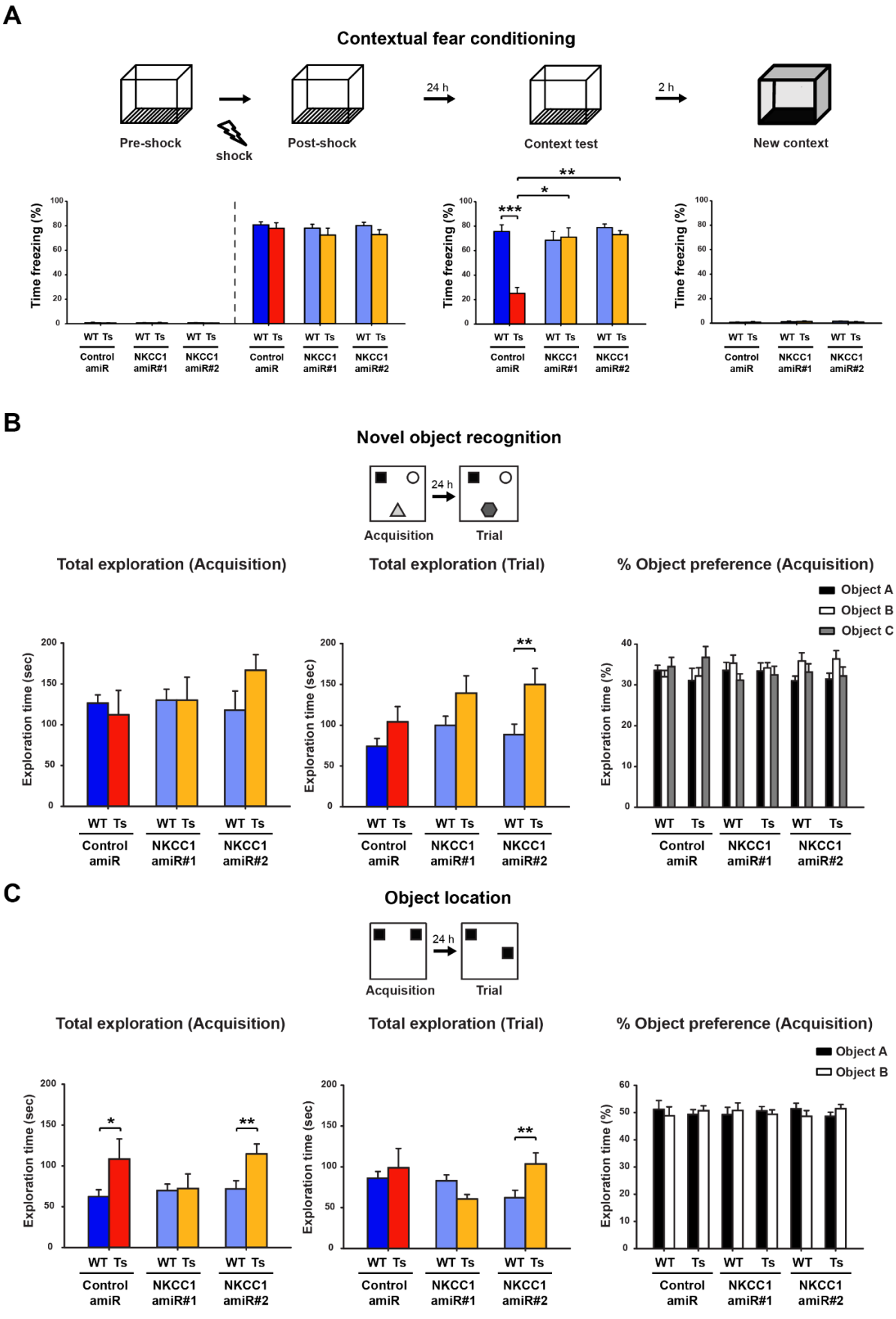
A
Contextual fear conditioning
Pre-shock
shock
Post-shock
24 h
Context test
2 h
New context
Time freezing (%)
WT Ts
Control amiR
NKCC1 amiR#1
NKCC1 amiR#2
B
Novel object recognition
24 h
Acquisition
Trial
Total exploration (Acquisition)
Total exploration (Trial)
% Object preference (Acquisition)
Exploration time (sec)
Exploration time (%)
Object A
Object B
Object C
C
Object location

Supplementary Figure 8. Effect of AAV_9 delivery of control and NKCC1 amiRs on behavioral tasks at 6 months post-injection. (A) *Left:* in the CFC test, brain AAV_9 delivery had no effect on the freezing time before (left) or immediately after (right) the electric foot shock during the conditioning session in both WT and Ts65Dn mice. *Center*: quantification of the freezing response in AAV_9-injected WT and Ts65Dn mice when re-exposed to the conditioning context (same data showed in Fig 5C). *Right:* both WT and Ts65Dn mice showed negligible freezing response when exposed to a new context. Control amiR: WT, *n* = 12; Ts65Dn, *n* = 7. NKCC1 amiR#1: WT, *n* = 12; Ts65Dn, *n* = 7. NKCC1 amiR#2: WT, *n* = 14; Ts65Dn, *n* = 13. **(B)** *Left*: in the NOR test the total exploration time during the acquisition phases was not significantly different across genotype and treatment. *Center*: the total exploration time during the trial phase was slightly increased in Ts65Dn mice injected with AAV_9 expressing NKCC1 amiR#2 compared to the corresponding WT animals. *Right*: the percentage of time spent exploring the three objects during the acquisition phase of the NOR test was not statistically different across the experimental groups. Control amiR: WT, *n* = 12; Ts65Dn, *n* = 7. NKCC1 amiR#1: WT, *n* = 12; Ts65Dn, *n* = 7. NKCC1 amiR#2: WT, *n* = 16; Ts65Dn, *n* = 13. **(C)** *Left*: in the OL test the total exploration time during the acquisition phase was slightly increased in Ts65Dn mice injected with AAV_9 expressing both control amiR and NKCC1 amiR#2 compared to the corresponding WT animals. *Center*: the total exploration time during the trial phase of the OL test was slightly increased in Ts65Dn mice injected with AAV_9 expressing NKCC1 amiR#2 compared to the corresponding WT animals. *Right*: the percentage of time spent exploring the two objects during the acquisition phase of the OL test was not statistically different across the experimental groups. Control amiR: WT, *n* = 12; Ts65Dn, *n* = 6. NKCC1 amiR#1: WT, *n* = 12; Ts65Dn, *n* = 6. NKCC1 amiR#2: WT, *n* = 15; Ts65Dn, *n* = 13. For all panels: **P*<0.05, ***P*<0.01, ****P*<0.001, Tukey *post hoc* test following two-way ANOVA.

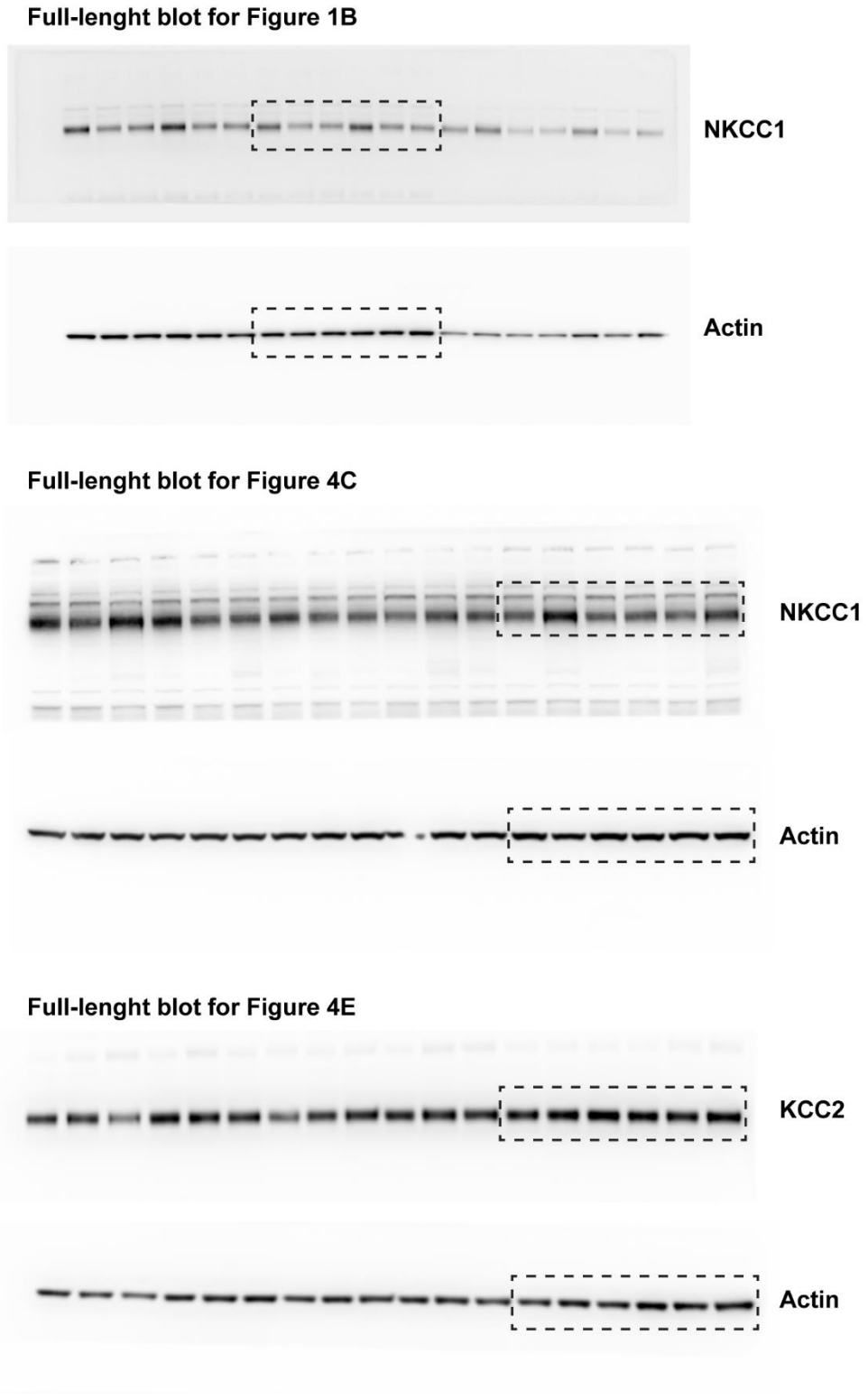

Supplementary Figure 9. Full-length blot images corresponding to the cropped western blot (dashed squares) presented in Figures 1B, 4C, 4E.